Available online at www.sciencedirect.com
SCIENCE DIRECT®
Journal of Magnetic Resonance 173 (2005) 54–63
JMR Journal of Magnetic Resonance
www.elsevier.com/locate/jmr

Numerical simulation of PRESS localized MR spectroscopy

Andrew A. Maudsley[a,*], Varanavasi Govindaraju[a], Karl Young[b,c], Zakaria K. Aygula[a], Pradip M. Pattany[a], Brian J. Soher[a,1], Gerald B. Matson[c,d]

[a] Department of Radiology, University of Miami School of Medicine, 1115 N.W. 14th St., Miami, FL 33136, USA
[b] Department of Radiology, University of California, San Francisco, USA
[c] Department of Pharmaceutical Chemistry, University of California, San Francisco, USA
[d] MR Unit, Department of Veterans Affairs Medical Center, San Francisco, CA 94121, USA

Received 4 August 2004; revised 11 November 2004
Available online 15 December 2004

Abstract

Numerical simulations of NMR spectra can provide a rapid and convenient method for optimizing acquisition sequence parameters and generating prior spectral information required for parametric spectral analysis. For spatially resolved spectroscopy, spatially dependent variables affect the resultant spectral amplitudes and phases, which must therefore be taken into account in any spectral simulation model. In this study, methods for numerical simulation of spectra obtained using the PRESS localization pulse sequence are examined. A comparison is made between three different simulation models that include different levels of detail regarding the spatial distributions of the excitation functions, and spin evolution during application of the pulses. These methods were evaluated for measurement of spectra from *J*-coupled spin systems that are of interest for in vivo proton spectroscopy and results compared with experimental data. It is demonstrated that for optimized refocusing pulses it is sufficient to account for chemical shift effects only, although there is some advantage to implementing a more general numerical simulation approach that includes information on RF pulse excitation profiles, which provides sufficient accuracy while maintaining moderate computational requirements and flexibility to handle different spin systems.

Keywords: In vivo proton MR spectroscopy; Press; Numerical simulation

1. Introduction

Biomedical applications of volume localized MR spectroscopy benefit from automated spectral analysis methods, and in particular those that incorporate prior spectral information to improve the accuracy and speed of the fitting procedure [1,2]. Young et al. [3,4] have previously reported that this prior spectral information can be derived using computer simulation methods to determine a set of basis functions that contain the relative amplitudes, phases, and frequencies of all resonances in each metabolite spectrum, based on measured *J*-coupling and chemical shift values. This approach provides a rapid and convenient alternative to experimental measurement of the individual spectral basis functions [2,5]; however, for accurate quantitation it is important that the simulation model accurately account for all physical parameters that may affect the resultant spectrum.

The point resolved spectroscopy (PRESS) method [6,7] is an example of an acquisition method where spatially dependent variables, such as the slice selection pulse shapes and gradient amplitudes, can result in differences of the resultant spectrum in comparison to that obtained by idealized RF pulses. This widely used localized acquisition method uses double spin-echo

* Corresponding author. Fax: +1 305 243 8099.
E-mail address: AMaudsley@med.miami.edu (A.A. Maudsley).
[1] Present address: Duke Image Analysis Laboratory, DUMC Box 3863, Durham, NC 27710, USA.

1090-7807/$ - see front matter © 2004 Elsevier Inc. All rights reserved.
doi:10.1016/j.jmr.2004.11.018

excitation sequence with each pulse providing spatial localization along an orthogonal direction. It can be described as (90°-τ_1-180°-τ_1-τ_2-180°-τ_2-Acq.), where $TE = 2(\tau_1 + \tau_2)$, and is termed a symmetric PRESS sequence when $\tau_1 = \tau_2$. The PRESS sequence is subject to a number of mechanisms that result in reduced signal intensities for coupled spins [8–15], and for spectral quantitation it is essential that these variations be accounted for. Previous reports have included detailed analyses of these effects using full density matrix treatments or product operator calculations, typically carried out for the AX_3 system of lactate, to aid in the understanding and modeling of spectral variations as a function of pulse sequence parameters. However, analytical methods become intractable for spin systems with more than two spin couplings [4] and for including realistic pulse shapes, making this approach difficult to implement as a general spectral simulation tool. These calculations are therefore most effectively implemented using numerical simulation methods. In this report, we address this requirement for prediction of spectra from *J*-coupled spin systems using PRESS volume selection with the aim of providing accurate a priori information to be used in a parametric spectral analysis procedure.

A convenient set of tools for performing numerical calculations of MR phenomena is provided by the GAMMA NMR simulation library [16]. The authors have previously described the use of this library for generating a priori information for use in a parametric spectral analysis procedure [3,4], and in this report, this approach is extended for analysis of the PRESS localization sequence. Since the purpose of this study is to develop numerical methods to calculate spectra from multiple metabolites in an efficient and accurate manner, a comparison of different models for the numerical simulation methods is made to compare the relative accuracy and computational requirements, for parameters typical of in vivo ^{1}H spectroscopy studies.

There are three primary mechanisms by which spatial selection parameters can lead to spectral variations of coupled spin systems, namely: the chemical shift offset artifact [8,12,17]; tip angle variations as a function of pulse profiles [15,18]; and spin evolution during the selection pulses [12]. For a complete simulation of the PRESS sequence, these must be considered along with the pulse sequence timings and other effects such as B_0 and B_1 inhomogeneity and spin relaxation. Numerical simulations of the PRESS sequence that demonstrate the three effects have been presented by Slotboom et al. [12], and by Thompson and Allen [14], though limited comparisons of the simulation methods or quantitative comparison with experimental results have been provided.

The chemical shift offset artifact arises from variations in the spatial distributions of the excitation functions for coupled spins pulses due to the chemical shift, which can result in phase variations leading to signal cancellation. The magnitude of this effect is a function of the chemical shift difference between coupled spins and the bandwidth and shape of the localizing pulse, which is typically limited by the strength of the available gradients and RF power. The simplest approach to model this effect is to assume ideal pulse rotations and to compartmentalize the localized volume, with each compartment representing a different combination of the two refocusing pulses for pulse angles of either 0° or 180°, for each of the chemically shifted spin multiplet groups of the coupled partners [8,17]. For coupling between two spins systems, as in lactate for example, there are 7 spatial compartments altogether, with 4 compartments for each spin of which the typically largest compartment is common to both spins and represents the correct refocusing sequence. In this report, we refer to this as the "4-compartment" model, though it should be noted that additional compartments must be considered if additional spin couplings are present.

The 4-compartment approach does not account for signal loss or generation of higher-order coherences due to pulse angle variations, and a refinement to this model must therefore account for the spatially dependent variations in the tip angle of the refocusing pulses. Experimental demonstrations of the considerable influence that the pulse shapes have on signal quantitation has been reported [13,19]. A simulation model that includes the tip angle profiles of the RF refocusing pulses will not only account for intensity variations across each of the compartments previously considered, but will also account for the transition bands at the edges of the compartments and possible excitation outside of the selected volume due to sidelobes. Although optimized pulse shapes can both reduce the tip angle variation across the selected region and out-of-volume excitation, it may still be beneficial to account for the signal contributions coming from the transition bands at the edges of all compartments. In addition, distortions to the expected excitation profile may occur due to non-linear characteristics of the RF transmitter section. These effects can be accounted for by incorporating the measured tip angle profiles in the simulation, which can be done by summing results obtained for multiple spatial locations spanning each slice-selection dimension. The result will depend on the accuracy with which the tip-angle profiles are mapped onto the selected volume, with a larger number of spatial points providing a more accurate representation of rapidly changing localization profiles, though at the cost of additional processing time.

A frequency selective RF pulse can be modeled as a series of small tip angle, ideal rotations, interleaved with short evolution periods that account for spin evolution occurring during the pulse [12,14]. While this more realistic model can be easily implemented, it requires a large increase in the computational requirement compared to

the 'hard pulse' assumption. Furthermore, it may provide no advantage over the simple hard-pulse excitation model if the value of $1/J$ is large compared to the length of the pulse, in which case J-evolution during the pulse is small [12]. This assumption is generally considered to be valid for ^{1}H metabolites [12], where pulse lengths may be on the order of 5×10^{-3} s and values of $1/J$, e.g. for lactate, are 144×10^{-3} s. However, some $1/J$ values may be smaller, as for aspartate CH_2 for which $1/J = 57 \times 10^{-3}$ s, [20], and it is unclear whether the simplified model still holds. Since the more realistic simulations are considerably more compute-intensive, it is instructive to examine which is most appropriate for a given set of sequence parameters and metabolites.

For this study, a series of simulations were performed for PRESS localization of ^{1}H metabolites that used each of the models described above, and results compared with experimental data for lactate, obtained at 1.5 and 7 T. In addition, two different excitation profiles of the 180° pulses are considered. Comparison of the accuracy and computational requirements of the models was made to determine which was most suitable for generation of a priori information for parametric modeling of J-coupled ^{1}H metabolites.

2. Methods

2.1. Spin systems

Spectral simulations and experimental measurements were performed for lactate, $CH_3CH(OH)CO_2^-$, an AX_3 spin system that has been widely used in previous studies due to its clinical relevance, its relatively large chemical shift between the coupled CH and the CH_3 groups that resonate at 4.09 and 1.31 ppm, respectively, and relative simplicity of the spin system. In addition, the CH_3 singlet resonance of acetate, at 1.90 ppm, was included as a reference signal.

To evaluate effects of phase evolution during the RF localization pulse, simulations were performed for aspartic acid, $^-O_2CCH_2CH(NH_2)CO_2^-$, an ABX spin system that includes a relatively large J-coupling between the non-equivalent protons of the CH_2 group of 17.4 Hz. The chemical shifts and J-coupling parameters obtained from previous measurements [20] were used.

2.2. Experimental methods

Spectra were acquired at 1.5 T (Philips, Edge) using symmetric and asymmetric PRESS acquisition sequences. Data and simulation results were obtained for two 180° refocusing pulses that had significantly different slice selection profiles. The first was an optimized pulse shape provided by the instrument manufacturer that provided a relatively sharp transition band with a bandwidth of 1.389 kHz and a pulse length of 6 ms. The second was a Gaussian-weighted Sinc function with a bandwidth of 1.399 kHz and pulse length of 1.7 ms. The resultant magnetization profiles for these two pulses are shown in Fig. 1.

To compare the relative amplitudes of the lactate doublet and acetate in the measured and simulated spectra, data were obtained at 1.5 T for each of the 180° refocusing pulse shapes. Measurements were obtained at several TE values using a PRESS selected volume of $2 \times 2 \times 2$ cm^3 within a spherical phantom (10 cm dia.) containing lactate (500 mM) and acetate (500 mM) in water. To compare simulation and experimentally measured signal ratios it was necessary to account for transverse relaxation, and the T_2 values for lactate and acetate were measured separately using the same metabolite solutions contained within a small spherical phantom (20 mm dia.). For lactate, spectra were obtained for TE values corresponding to multiples of $1/J$ of the lactate doublet, up to TE = 576 ms, and the results of spectral fitting of the doublet then fitted to a single exponential decay function.

Spectral processing and analysis of the acquired spectra were implemented using in-house software. This included 2 Hz exponential smoothing, baseline correction, and calculation of the relative intensities of the acetate resonance and the lactate doublet by both spectral integration and by spectral fitting using HLSVD [22].

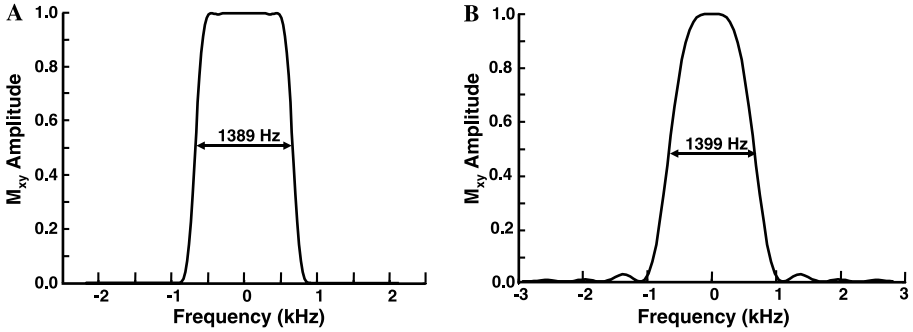

Fig. 1. Excitation profiles of the 180° refocusing pulses used for the PRESS simulations and measurements obtained at 1.5 T.

To illustrate the spectral variation that occurs over the selected volume, a spectroscopic imaging (SI) acquisition was obtained at 7 T (SMIS) using PRESS volume selection with an optimized pulse shape [21] of 3 kHz bandwidth and 4.019 ms pulse length. Data were obtained using a spherical phantom (20 mm dia.) containing lactate (500 mM) and acetate (83.3 mM) in D_2O, for TE = 288 ms, TR = 4 s, 8192 sample points, PRESS volume of $5\times5\times3\,mm^3$, FOV of 8×8 mm, and 32×32 phase encoding measurements over the two spatial dimensions corresponding to the 180° refocusing pulses. Data reconstruction included mild Gaussian spatial smoothing and exponential filtering in the time domain corresponding to 2 Hz line broadening. Spectroscopic images were then obtained by spectral integration over each multiplet group.

2.3. Simulation methods

Numerical simulation of the symmetric PRESS sequence was carried out for lactate and acetate, using: (1) the 4-compartment model; (2) the tip-angle profile model; and (3) the complete pulse simulation model. All programs were written in C++ using calls to the GAMMA library [16], via a user and database interface written using IDL (Research Systems). In all models, an ideal 90° excitation pulse was assumed. An example of the GAMMA code for the tip-angle profile model is provided in the Appendix. The simulation code for the tip-angle profile model is included in a general spectral simulation package [23] that is available on request.

For the 4-compartment model, the chemical shift offset effect for lactate was accounted for as described by Yablonskiy et al. [17]. A numerical simulation was performed for each of the 4 regions for the lactate doublet, that correspond to different combinations of the two 180° localization pulses acting on the CH and CH_3 groups, and the resulting set of transition frequencies, amplitudes, and phases added with a weighting determined by the relative size of each sub-region [8,17,24]. The size of each region was determined by the chemical shift separation, gradient strength, and bandwidth of the refocusing pulses. It should be noted that the GAMMA implementation includes the complete spin Hamiltonian, whereas the analytical formula used in the earlier report [17] was a vector model that did not account for polarization transfer effects. The simulation for acetate was performed for a single compartment, and weighted by the size of the PRESS-selected volume (i.e., 16 ml).

To implement the remaining two models, the numerical simulation was repeated over an array of $N\times N$ points spatially distributed over an area twice the size of the PRESS selected volume (defined at full width at half maximum), and containing all compartments selected for all coupled spins. The region over which the simulation was carried out is referred to as the field of view (FOV). Examination of the RF excitation profiles indicated that the rotation angles, and hence resultant signal contributions, were negligible outside of the FOV. The final spectrum was then obtained by combining the simulation results obtained at all points and scaling by the total number of points. Some reduction of processing time was obtained by not performing the calculation for any location that corresponded to a rotation angle of less than 1°.

The choice of the spatial array size must consider a trade-off of accuracy and computation time. Larger values will improve the ability to account for signals originating within the rapidly varying transition bands of the localization pulses but will increase the computation time. Although computation times are generally modest for the hard pulse excitation assumption, this nevertheless becomes an important consideration when the intended application is to obtain a priori information for multiple metabolites, some of which include multiple spin couplings, for multiple experimental parameters. To determine the optimal value for this spatial sampling, the tip-angle profile model was simulated for values of N from 4 to 120, for the symmetric PRESS sequence at 1.5 T with TE = 288 ms, and the vector-summation of the transition values corresponding to the lactate doublet and quartet groups, and the acetate singlet were plotted. To reduce processing time the acetate CH_3 group was defined using a single proton only and the result multiplied by three.

For the tip-angle profile model, a hard pulse excitation is assumed for each refocusing pulse, but using the rotation angle corresponding to each spatial location in each dimension as determined from the excitation profile. The chemical shift offset was modeled by varying the effective spatial position according to the chemical shift of the spin, σ_{spin}. Therefore, for a spatial location, (x,y), an effective position, (x',y'), was calculated as:

$$x' = x + \frac{\sigma_{spin} - \sigma_{ref}}{\gamma G_x} \quad \text{and} \quad y' = y + \frac{\sigma_{spin} - \sigma_{ref}}{\gamma G_y}, \qquad (1)$$

where G_x and G_y are the applied gradients and σ_{ref} is the spectrometer reference frequency. For these studies, σ_{ref} was chosen to correspond to the average of the lactate CH and CH_3 chemical shifts. For each dimension, these effective spatial locations were then mapped onto the spatial localization profiles to obtain the pulse angles of the two refocusing pulses.

The refocusing excitation profiles were obtained by first generating the resultant complex magnetization profile, M_{xy}, using the Bloch equations as implemented in Matpulse [21], and converting this to a spatially variant rotation angle, $\theta(r)$, using the relation $\theta(r) = \text{acos}(1–2M_{xy})$ [21,25]. This spatial excitation profile was defined using 300 points, which were then mapped onto the N points used to cover the FOV using linear

interpolation. The resultant magnetization profiles obtained from: (a) the Bloch simulation result for a 180° refocusing pulse; (b) the profile through the center of the PRESS-SI simulation result for a singlet resonance obtained using the tip-angle profile simulation model; and (c) the corresponding profile obtained using the complete time-domain RF pulse simulation model; all showed excellent agreement. The same pulse shape and parameters were used for both refocusing pulses.

To confirm the implementation of the tip-angle profile model, the simulation was also performed using an idealized excitation profile, consisting of an exact 180° rotation over the specified bandwidth and zero outside, and the results were compared to the analytical result for the 4-compartment model [17].

The PRESS sequence includes dephasing and rephasing gradient pulses around each 180° pulse to eliminate magnetization from outside of the selected region and higher-order coherences, while refocusing the desired magnetization, which must be accounted for in the tip-angle profile and the complete pulse simulation models. A common method for performing this calculation is to assume a semi-continuous distribution of spins over each sub-volume in the spatial array, and to repeat the simulation for multiple locations distributed over that volume [26,27]. Summation of the resultant spectra then obtains the desired signal cancellation or refocusing. This procedure can be implemented using the density matrix approach by applying a transverse phase rotation operator, equivalent to assuming different spectrometer frequencies for the time of the applied gradient; however, this approach can be very time consuming since several hundred repetitions may be necessary. Therefore, a more efficient 4-phase simulation was implemented similar to that previously described for removal of unwanted coherences in the STEAM sequence [4]. For each 180° refocusing pulse the simulation was repeated four times, using phase rotations of 0, π/2, π, and 3π/2, both prior to, and following, application of the 180° pulse operator. This model was verified by comparison with results obtained for larger number of repetitions, with phases equally distributed over 2π.

The most general simulation, termed the complete-pulse simulation model, was obtained by numerical calculation of the spectrum at each spatial location using the complete refocusing pulse in the time domain and accounting for *J*-coupling spin evolution during the pulse. The GAMMA package accomplishes this by the application of a series of ideal pulses followed by short inter-pulse evolution periods. The pulse can be specified in as much detail (i.e., time resolution) as desired with more detail obviously resulting in higher computational cost. For this study, all pulse shapes were defined using 256 time points. The spatial location across the $N \times N$ points was modeled as a shift of the spectrometer reference frequency during the refocusing pulse corresponding to the effective spatial location, e.g., for the x dimension as:

$$\omega_x = f_0 \cdot \sigma_{\text{ref}} + \gamma \cdot G_x \cdot \text{FOV} \cdot n_x/N, \quad (2)$$

where the index $n_x = -N/2 \cdots N/2 - 1$, and f_0 is the resonance frequency corresponding to $\sigma_{\text{ref}} = 0$ ppm.

Spectra were simulated using all three models for an asymmetric PRESS measurement at several TE values, with τ_1 fixed at a value of 21 ms. Results were compared with experimental acquisitions by evaluating the relative amplitudes of the acetate singlet resonance to the signal integral from the lactate doublet, while accounting for the T_2 signal loss for these resonances. Signal integrals were obtained using vector summation of transition intensities obtained from the simulation studies and by spectral fitting of the experimental data.

A simulation study was carried out for the symmetric PRESS-SI measurement at 7 T with TE = 288 ms, using the tip-angle profile model with the same parameters as for the experimental measurement. Spectroscopic images were created by simulating spectra over a 32×32-point array, corresponding to the experimentally obtained SI data, with a 1.0 Hz Gaussian line broadening applied. To improve visual comparison with the experimentally obtained data, the simulated images were convolved in the spatial domain with a smoothing kernel equal to the *k*-space apodization function applied to the experimental data.

To investigate whether it was necessary to account for the effect of *J*-coupling evolution occurring during the localization pulses, a simulation study was carried out for observation of aspartate using the tip-angle profile model and the complete pulse model, using symmetric PRESS at several TE values, and the results compared.

3. Results

In Fig. 2 are shown experimental and simulation results for the PRESS-SI study of lactate at 7 T, both obtained using the optimized 180° pulse shape. Images derived from the lactate doublet and quartet multiplet groups are shown, in which the multiple compartments within the PRESS-selected volume can be clearly identified. Also shown are spectra selected from single voxels located within each compartment. The simulation result demonstrates excellent agreement of the image amplitude distribution as well as relative phases of the experimental and simulated spectra.

In Fig. 3 are shown the integrated signal results for the simulated PRESS spectrum plotted as a function of the number of points used to describe the FOV in each spatial dimension. The tip-angle profile model was used with the optimized 180° pulses, TE = 288 ms, and at 1.5 T. Plots are shown for the reference singlet,

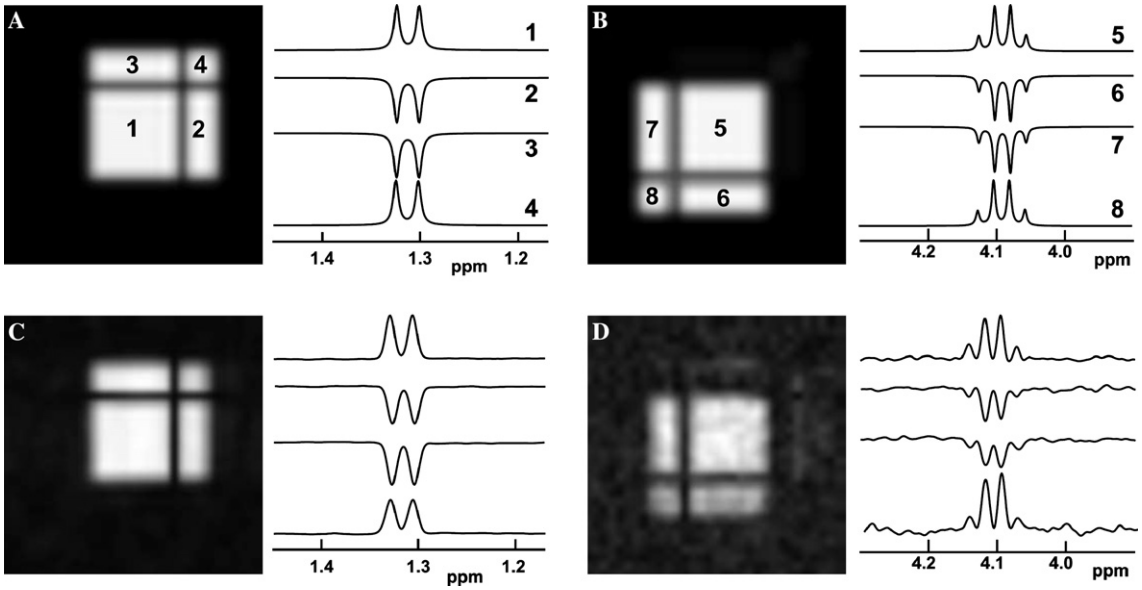

Fig. 2. Comparison of spectroscopic images and spectra obtained for PRESS observation of lactate by computer simulation using the tip-angle profile model (A,B) and experimental measurement (C,D). Results are shown for 7 T measurement and TE = 288 ms. (A,C) Data from the CH_3 doublet resonance. Images are obtained by integration of the signal magnitude over 0.8–1.8 ppm, and the spectra are selected from each of the 4 regions as indicated; (B,D) the corresponding results for the CH quartet.

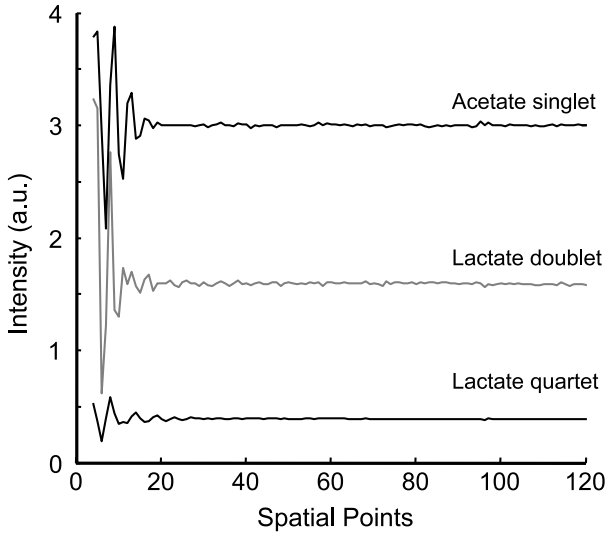

Fig. 3. Integrated signal intensities for the PRESS simulation using the tip-angle profile model, plotted as a function of the number of points used to define the FOV in each dimension. Data are shown for measurement at 1.5 T with TE = 288 ms, for the acetate singlet, the lactate doublet, and quartet.

and the lactate doublet and quartet signals. The results indicate that considerable errors in the integrated signals are obtained if an inadequate spatial sampling density is used. For the doublet and quartet signals, as well as the ratio of these values, and for the same results obtained using the complete-pulse model (data not shown), minimal difference of the simulated intensities is obtained for N greater than 40 points. For the simulations presented in the remainder of this study, a value of $N = 64$ was used for the tip-angle profile model and the complete pulse simulation model.

Fig. 3 also illustrates the considerable signal loss that can occur for PRESS observation of lactate. Keeping in mind that the doublet is derived from three spins (i.e., could have maximum relative amplitude of 3.0) it can be seen that the resultant signal is only 60% of that available, illustrating the importance of accounting for these effects in signal quantitation. The detected signal typically decreases with field strength, becoming 20% for our 7 T simulation parameters, though is less for coupled spin systems that have a smaller chemical shift difference.

The ratios of integrated area of the lactate doublet relative to the acetate singlet reference, for measurements and simulations of the symmetric PRESS sequence at 1.5 T, are shown in Table 1, for data obtained using both the optimized and Sinc refocusing pulse shapes. The effect of T_2 losses was removed from the experimental results, with T_2 values for acetate and the lactate doublet determined to be 2500 and 833 ms, respectively. The approximate times required for the tip-angle profile model and the complete pulse simulation model were 10 and 180 min, respectively, for 64×64 points across the FOV (Intel, 2 GHz processor). Good agreements between experimental and simulation results were obtained from all simulation models at both TE values for the optimized pulse profile, though larger differences are seen for the poorer pulse profile, with the largest discrepancy seen for the complete pulse model at TE = 288 ms.

Table 1
Ratio of the integrated signal intensity from the lactate doublet relative to the reference acetate singlet, for each of the simulation models and experimental data, at 1.5 T

Model	Optimized 180°		Sinc 180°	
	TE = 144 ms	TE = 288 ms	TE = 144 ms	TE = 288 ms
Analytical 4-compartment	−0.738	0.541	−0.739	0.544
Tip-angle profile model	−0.747	0.520	−0.690	0.309
Complete pulse model	−0.739	0.528	−0.655	0.269
Experimental data	−0.738	0.537	−0.634	0.456

The experimental results have been corrected for the effect of the different T_2 values.

The additional simulation performed using the tip-angle profile model for the idealized refocusing pulse (i.e., with perfect refocusing pulse angle over the entire selected volume) at TE = 144 ms points obtained a Lac/Ace ratio of −0.736, which was in good agreement with the analytical result using the 4-compartment model of −0.738.

Experimental and simulation results obtained using the asymmetric PRESS sequence with the optimized pulse shape for a range of TE values are shown in Fig. 4. Simulation results are shown for all three models, calculated at the measured TE times, and for the four-compartment and pulse-angle profile models calculated for a larger number of TE values. Experimental data were obtained by spectral fitting of the lactate doublet and correcting for the T_2 decay. Good agreement between the data and all simulation results can be seen. Careful inspection reveals that the four-compartment model result also includes small high-frequency oscillations that arise from polarization transfer effects [24], which differs from the analytical treatment previously used for this model [17]. Although these oscillations are weak in the asymmetric PRESS sequence used for this example, they have a much stronger effect for the symmetric PRESS sequence and can lead to much larger errors for the poorer pulse profile if not taken into account.

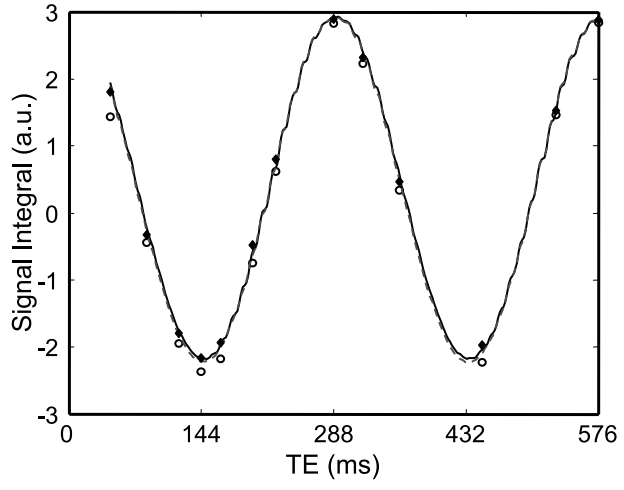

Fig. 4. Integrated signal from the lactate doublet as a function of TE value for an asymmetric PRESS sequence. Data are shown for: (a) the experimental measurement (circles), (b) the four-compartment simulation model (dashed line); (c) the tip-angle profile simulation model (solid line); and (d) selected TE values for the complete pulse simulation model (solid diamonds).

Simulations for the PRESS measurement of aspartate, for TE values of 25 and 100 ms obtained using the pulse-angle profile and the complete pulse simulation models showed identical results (data not shown). This confirms that effects of *J*-coupling during the spatially selective excitation pulses can be ignored for simulation of ^{1}H spectra.

4. Discussion

This study indicates that for numerical simulation of a symmetric PRESS sequence using the optimized refocusing pulse profiles and TE values at increments of $1/J$, all simulation models result in good agreement with the experimental data; however, results for the poor excitation profiles demonstrated much greater disagreement between simulation and experimental results. For both pulse shapes and TEs examined, the results for the 4-compartment model were in good agreement with experimental results. One possible explanation for this somewhat surprising finding is that the errors in the spatial selection profiles effectively cancel, i.e., the area of reduced positive signal (e.g., in region 1 of Fig. 2A) is equivalent to the reduced negative signal regions (regions 2 and 3 of Fig. 2A). However, the relative performance for more complex spin systems has not been demonstrated. An additional advantage of the more general simulation approach is that it is easily generalized, i.e., the same program can be applied to any spin system and can be readily modified for any pulse sequence, whereas the 4-compartment model would need to be reformulated for each spin system.

Our results indicate that for ^{1}H metabolites consisting of small numbers of spins it is unnecessary to use the more computationally intensive complete pulse model to account for *J*-coupling evolution during the selective pulses and that the tip-angle profile model provides accurate results while requiring reasonable computational requirements. It is speculated that the larger discrepancies for the poor excitation profile may be a

result of small differences between the experimental pulse shapes or rotation angles from the simulation, which result in significant signal differences over the relatively broad transition band regions; however, the reason for this discrepancy has not been determined.

This study was initially implemented using measurements obtained at 7 T; however, it was observed that the larger B_0 inhomogeneity caused difficulties for making the metabolite ratio measurements. Whereas the spatially dependent alterations of spectra from *J*-coupled resonance groups normally result in changes in amplitude only, in the presence of lineshape, phase, and spin density variations over the different spatial compartments, which are common for in vivo studies, the co-addition of these signal contributions will result in additional lineshape distortions and amplitude variations. An additional observation is that in this situation lineshape deconvolution [28] methods may be ineffective, since the reference signal likely originates from a different spatial region and may therefore have a different lineshape. Similarly, spectral fitting methods that assume a common resonance lineshape will be subject to errors.

5. Conclusions

A comparison of three models for numerical simulation of the PRESS volume localization method for ^{1}H spectroscopy has been presented. Results indicate that the simpler four-compartment model works well for the AX_3 spin system; however, the tip-angle profile model can perhaps be most easily generalized to support multiple spin systems and RF pulse designs. Results also indicate that for commonly observed ^{1}H metabolites it is not necessary to account for phase evolution occurring during the RF pulse. For the tip-angle profile model, the simulation must include a sufficient sampling density for the spatial distribution of the refocusing pulse profile to ensure an accurate result. For the localization profiles used in this study we have used 64 points over a FOV that was 100% larger than the selected region. The accuracy of the simulation method for generating basis functions in an automated parametric spectral analysis procedure has been demonstrated. While the current implementation does not consider variation of the excitation or reception sensitivity, or differences in relaxation rates of the coupled spin multiplet groups, these refinements could be added if necessary.

This study has also illustrated some disadvantages of the PRESS localization method that become significant for observation of coupled spin systems when chemical shifts between coupled spins become comparable to the excitation bandwidths, as is common for measurements at high fields. First, there can be a large signal loss caused by subtraction of signal in regions with negative phase. Second, variation of frequency, phase, and spin density across the PRESS localized compartments can lead to different lineshapes for each chemically shifted resonance group. Although resonance integrals are unaffected, this can lead to difficulties for quantitation.

Acknowledgments

This work was supported by PHS Grants EB00207 and EB0730. We thank Dr. James Murdoch for providing information on the optimized pulse shape design on the Philips/Edge MR system.

Appendix

Pseudocode for the tip-angle profile model for numerical simulation of PRESS, based on the GAMMA simulation code.

```
// Read tip-angle profiles.
read_profile (y_profile); read_profile (x_profile);
// Set up the spin system.
spin_system sys ("lactate.sys");
gen_op H = Hcs (sys) + HJ (sys);    // Construct static Hamiltonian.
gen_op sigma_total = sigma_eq (sys); // Construct total density operator.
gen_op detect = Fm (sys);            // Construct detection operator.
// Construct delay propagators.
TimeDelays[3] = {TE1/2., (TE1 + TE2)/2., TE2/2.};
gen_op UDelays[3];
for (i = 0; i < 3; i++) {UDelays[i] = prop(H, TimeDelays[i]);}
// For each spin, calculate the spatial shift (in mm) due to the chemical shift
// difference from the carrier frequency, for a gradient 'Grad' (in Hz/mm).
for (i = 0; i < sys.spins(); i++)
       spatial_shift[i] = (sys.PPM(i)-CS_OFFSET)*sys.Omega()/Grad;
```

```
// MAIN LOOP - for all X and Y
for (xpt = 0; xpt < NX; xpt++) {
  for (ypt = 0; ypt < NY; ypt++) {       // Spatial points across the FOV.
    sigma = sigma_eq (sys);                 // Setup equilibrium magnetization.
    sigma = Ixpuls (sys, sigma, 90.0);    // Apply initial excitation.
    sigma = evolve (sigma, UDelays[0]);    // Evolve spins fo TE1/2.
    for (Npulse = l; Npulse < 3; Npulse++) {// Loop over 180 RF pulses.
      // Split density operator into 4 dephased components.
      gen_op sigma_mx[4];
      // Apply the first dephasing gradient to all 4 components
      for (i = 0; i < 4; i++) sigma_mx[i] = evolve(sigma, Rz(sys, 90.0*i));
      // Apply RF pulse rotation to each phase component and spin, for
      // an effective location and RF pulse angle.
      for (nd = 0; nd < 4; nd++) {
        for (Nspin = 0; Nspin < sys.spins(); Nspin++) {
          if (Npulse = = l) {  // Parameters for first 180, in X.
            effpos = x_min + xpt * X_STEP + spatial_shift[Nspin];
            effangle = effective_angle (x_prof, effpos);}
          if (Npulse = = 2) {  // Parameters for second 180, in Y.
            effpos = y_min + ypt * Y_STEP + spatial_shift[Nspin];
            effangle = effective_angle (y_prof, effpos);}
            sigma_mx[nd] = Ixpuls(sys, sigma_mx[nd], Nspin, effangle);
        } // End of (Nspin) loop.
      } // End of (nd) loop.
      // Apply the second dephasing gradient.
      for (i = 0; i < 4; i++) sigma_mx[i] = evolve(sigma_mx[i], Rz(sys, -90.0*i));
      sigma = average (sigma_mx) // Merge the 4 dephased subsystems.
      zero_mqc (sys, sigma, 2, 1); // Keep ZQC and SQC.
      sigma = evolve (sigma, UDelays[Npulse]);
    }// End of (Npulse) loop.
    sigma_total + = (sigma / (NX*NY)); // Add results over the FOV.
  } // End of (ypt) loop.
} // End of (xpt) loop.
```

References

[1] A.A. De Graaf, W.M.M.J. Bovee, Improved quantification of in vivo 1H NMR spectra by optimization of signal acquisition and processing and by incorporation of prior knowledge into the spectral fitting, Magn. Reson. Med. 15 (1990) 305–319.

[2] S.W. Provencher, Estimation of metabolite concentrations from localized in vivo proton NMR spectra, Magn. Reson. Med. 30 (1993) 672–679.

[3] K. Young, V. Govindaraju, B.J. Soher, A.A. Maudsley, Automated spectral analysis I: formation of a priori information by spectral simulation, Magn. Reson. Med. 40 (1998) 812–815.

[4] K. Young, G.B. Matson, V. Govindaraju, A.A. Maudsley, Spectral simulations incorporating gradient coherence selection, J. Magn. Reson. 140 (1999) 146–152.

[5] A.A. De Graaf, J.E. van Dijk, W.M.M.J. Bovee, Quality: quantification improvement by converting lineshapes to the Lorentzian type, Magn. Reson. Med. 13 (1990) 343–357.

[6] R.E. Gordon, R.J. Ordidge, Volume selection for high resolution NMR studies, in: Proceedings of the Society of Magnetic Resonance in Medicine, New York, 1984, pp. 272–273.

[7] P.A. Bottomley, Spatial localization in NMR spectroscopy in vivo, Ann. N. Y. Acad. Sci. 508 (1987) 333–348.

[8] G. McKinnon, P. Boesiger, Lactate signal loss with echo based volume selective spectroscopy, Magn. Reson. Med. Biol. 4 (1990) 101–111.

[9] T. Ernst, J. Hennig, Coupling effects in volume selective 1H spectroscopy of major brain metabolites, Magn. Reson. Med. 21 (1991) 82–96.

[10] W.-I. Jung, O. Lutz, Localized double-spin-echo proton spectroscopy of weakly coupled homonuclear spin systems, J. Magn. Reson. 96 (1992) 237–251.

[11] A.H. Wilman, P.S. Allen, An analytical and experimental evaluation of STEAM versus PRESS for the observation of the lactate doublet, J. Magn. Reson. B101 (1993) 102–105.

[12] J. Slotboom, A.F. Mehlkopf, W.M.M.J. Bovee, The effects of frequency-selective RF pulses on J-coupled spin-1/2 systems, J. Magn. Reson. A108 (1994) 38–50.

[13] F. Schick, T. Nägele, U. Klose, O. Lutz, Lactate quantification by means of press spectroscopy—influence of refocusing pulses and timing scheme, Magn. Reson. Imag. 13 (1995) 309–319.

[14] R.B. Thompson, P.S. Allen, Sources of variability in the response of coupled spins to the PRESS sequence and their potential impact on metabolite quantification, Magn. Reson. Med. 41 (1999) 1162–1169.

[15] W.I. Jung, M. Bunse, O. Lutz, Quantitative evaluation of the lactate signal loss and its spatial dependence in press localized 1H NMR spectroscopy, J. Magn. Reson. 152 (2001) 203–213.

[16] S.A. Smith, T.O. Levante, B.H. Meier, R.R. Ernst, Computer simulations in magnetic resonance. An object-oriented programming approach, J. Magn. Reson. A106 (1994) 75–105.
[17] D.A. Yablonskiy, J.J. Neil, M.E. Raichle, J.J. Ackerman, Homonuclear J coupling effects in volume localized NMR spectroscopy: pitfalls and solutions, Magn. Reson. Med. 39 (1998) 169–178.
[18] J.M. Wild, R.B. Thompson, P.S. Allen, Automated quantitative spectroscopic imaging of coupled spins at 3T—influence of realistic volume selective pulse sequences, in: Proceedings of the International Society for Magnetic Resonance in Medicine, 2000, p. 1847.
[19] L.N. Ryner, Y. Ke, M.A. Thomas, Flip angle effects in STEAM and PRESS—optimized versus Sinc RF pulses, J. Magn. Reson. 131 (1998) 118–125.
[20] V. Govindaraju, K. Young, A.A. Maudsley, Proton NMR chemical shifts and coupling constants for brain metabolites, NMR Biomed. 13 (2000) 129–153.
[21] G.B. Matson, An integrated program for amplitude-modulated RF pulse generation and re-mapping with shaped gradients, Magn. Reson. Imag. 12 (1994) 1205–1225.
[22] W.W.F. Pijnappel, A. van den Boogaart, R. de Beer, D. Van Ormondt, SVD-based quantification of magnetic resonance signals, J. Magn. Reson. 97 (1993) 122–134.
[23] Z. Aygula, B.J. Soher, K. Young, A.A. Maudsley, GAVA—a graphical pulse sequence simulation, display and storage environment, in: Proceedings of the International Society of Magnetic Resonance in Medicine, Toronto, 2003, p. 852.
[24] R.A. de Graaf, D.L. Rothman, In vivo detection and quantification of scalar coupled 1H NMR resonances, Concepts Magn. Reson. 13 (2000) 32–76.
[25] J. Pauly, P. Le Roux, D. Nishimura, A. Macovski, Parameter relations for the Shinnar-Le Roux selective excitation pulse design algorithm, IEEE Trans. Med. Imag. 10 (1991) 53–65.
[26] G.H. Meresi, M. Cuperlovic, W.E. Palke, J.T. Gerig, Pulsed field gradients in simulations of one-and two-dimensional NMR spectra, J. Magn. Reson. 137 (1999) 186–195.
[27] R.B. Thompson, P.S. Allen, Response of metabolites with coupled spins to the STEAM sequence, Magn. Reson. Med. 45 (2001) 955–965.
[28] G.A. Morris, H. Barjat, T.J. Horne, Reference deconvolution methods, Prog. NMR Spectrosc. 31 (1997) 197–257.